DOI 10.1007/s10778-023-01192-3
International Applied Mechanics, Vol. 58, No. 6, November, 2022

STRESS STATE AND STRENGTH OF THIN-WALLED STRUCTURES UNDER NONISOTHERMAL RELOADING

M. O. Babeshko, A. Z. Galishin, and V. G. Savchenko

A method of numerical analysis of temperature fields and thermoelastoplastic stress–strain state of thin shells with assessment of strength under repeated loading is proposed. The modified constitutive equations of the theory of deformation along paths of small curvature are used, taking into account the perfect Bauschinger effect. A numerical example is given.

Keywords: thermoelastoplastic stress–strain state, thin shell, nonisothermal deformation process, strength, repeated loading

Introduction. Structural members are often modeled by thin isotropic shells of revolution. During operation under variable nonisothermal load, there may occur inelastic strains, which significantly affect their strength. The strength of the structure depends on many factors that accompany nonisothermal loading, such as the temperature dependence of the material characteristics, plastic and creep strains, deformation history, material damage, etc. When determining the optimal operating modes and predicting the strength of structures, it is necessary to determine their elastoplastic stress–strain state (SSS) taking into account real operating conditions. To this end, it is necessary to create methods for numerical analysis of the SSS of thin shells using the equations of state that describe the inelastic deformation of materials, and various approaches for assessing the strength of structures. There are developments aimed at creating mathematical models for predicting the critical load for thin-walled structures under different operating conditions. A method for determining the elastoplastic SSS and assessing the strength of a shell structure under increasing internal pressure is described in [20]. Methods for predicting the operational and limiting state of critical elements of rocket equipment under repeated thermomechanical loading with constant parameters are described in [21], where the number of repetitions to fracture is predicted as well. In contrast to [20, 21], we will address methods for determining the axisymmetric SSS and the critical load of structural members in the form of thin shells under repeated thermomechanical loading with parameters slightly changed compared with the previous load.

1. Problem Statement. When solving this problem, we will use the following basic assumptions:

– the meridian of the shell of revolution consists of links of different geometry;

– the shell is under axisymmetric thermomechanical loading;

– the geometrical dimensions of the shell and the load are such that it is possible to use the geometrically linear theory of shells with the Kirchhoff–Love hypotheses;

– the geometry of the shell and the load are such that the shell does not buckle;

– the thermomechanical loading in such that it can be considered as a set of successive equilibrium processes, and the deformation of the shell elements does not affect its temperature, i.e. the loading process is quasistatic and uncoupled;

– the shell deforms both within and beyond the elastic range at small strains;

– the creep strains are much smaller than the elastic and plastic strains and can be neglected;

– unloading (either partial or complete) and secondary plastic strains may occur in plastic ranges;

– the behavior of the material can be described by the perfect Bauschinger effect;

S. P. Timoshenko Institute of Mechanics, National Academy of Sciences of Ukraine, 3 Nesterova St., Kyiv, Ukraine, 03057; e-mail: plast@inmech.kiev.ua. Translated from Prykladna Mekhanika, Vol. 58, No. 6, pp. 70–83, November–December 2022. Original article submitted November 09, 2021.

1063-7095/22/5706-0683 ©2022 Springer Science+Business Media, LLC

– unloading in the shell elements can occur due to not only a reduction in the external load, but also a change in temperature.

Let the stress- and strain-free shell at temperature $T = T_0$ be subjected to axisymmetric mechanical loads and uneven heating at the initial time $t = 0$. To determine the SSS of the shell during deformation, the loading process is divided into a number of stages so that the moments of division are as close as possible to the moments of transition from active loading to possible unloading and back. At each stage, it is necessary to know the loads, the boundary conditions, and the distribution of temperature over the meridional section. This means that the problem of thermoplasticity is reduced to the determination of the temperature distribution in the shell (thermal conduction problem), followed by the determination of the SSS at known temperatures and mechanical loads. The problem of thermoplasticity at each stage is solved by the method of successive approximations, after which it is necessary to test the failure criteria. If one of the criteria is satisfied, then the load at this stage is considered destructive.

The shell is described in a curvilinear coordinate system s, θ, ς fixed to an undeformed continuous coordinate surface, where s ($s_a \le s \le s_b$) is the meridional coordinate; s_a, s_b are the coordinates of the ends of the shell; ς ($\varsigma_0 \le \varsigma \le \varsigma_k$) is the coordinate reckoned along the normal to the coordinate surface; ς_0 and ς_k refer to the inner and outer surfaces, respectively; shell thickness $h = \varsigma_k - \varsigma_0$. Let the midsurface or one of the surfaces of the shell be the coordinate surface.

Thus, at any stage of loading, we solve the thermal conduction problem to find the temperature distribution over the meridional section $T(s, \varsigma)$ and then we determine the components of the stress σ_{ij} and strain ε_{ij} tensors.

2. Thermal Conduction Problem. The temperature field of the shell is determined by solving the nonstationary heat conduction problem. In the chosen coordinate system, the thermal conduction equation for thin shells under axisymmetric heating can be written in the following form [1, 5]:

$$\frac{\partial T}{\partial t} = a(F^{(s)} + F^{(\varsigma)}), \tag{1}$$

$$F^{(s)} = \frac{\partial^2 T}{\partial s^2} + \left(\frac{1}{\lambda}\frac{\partial \lambda}{\partial s} + \rho\right)\frac{\partial T}{\partial s},$$

$$F^{(\varsigma)} = \frac{\partial^2 T}{\partial \varsigma^2} + \left(\frac{1}{\lambda}\frac{\partial \lambda}{\partial \varsigma} + k\right)\frac{\partial T}{\partial \varsigma}, \tag{2}$$

where $a = a(T)$, $\lambda = \lambda(T)$ are thermal diffusivity and thermal conductivity coefficients; $k = k_s + k_\theta = \dfrac{d\varphi}{ds} + \dfrac{\sin\varphi}{r}$ is the sum of the principal curvatures of the coordinate surface; $\rho = \dfrac{\cos\varphi}{r}$; $r = r(s)$ is the radius of the coordinate surface; $(\pi - \varphi)$ is the angle between the normal to the coordinate surface and the axis of revolution z.

The solution to Eq. (1) must satisfy the boundary conditions on the shell surface [2, 17]. The boundary conditions of convective heat exchange with the environment were addressed in [1]. In contrast to [1], we will consider the heating of the shell by a given heat flux, convective and radiant heating, or their combination [12]. In the general case, the boundary conditions on the surface of the shell with external normal $\vec{n}$ have the form

$$\frac{\partial T}{\partial n} = -\frac{1}{\lambda}\Big[\alpha(T - \Theta) + C\breve{\varepsilon}(T^4 - \Theta^4) - q\Big] = -\frac{A}{\lambda}, \tag{3}$$

where α is the heat-transfer factor; Θ is the environment temperature; $C = 5.67 \cdot 10^{-8}$ W/(m^{2}K^4) is the Stefan–Boltzmann constant; $\breve{\varepsilon}$ is the emissivity factor; q is the given heat flux. The type of boundary conditions on the surface of the shell depend on the values of α, $\breve{\varepsilon}$, q. On the surfaces bounding the shell, conditions (3) have the form

$$\text{if} \quad \varsigma = \varsigma_0, \quad \text{then} \quad \frac{\partial T}{\partial \varsigma} = \frac{\alpha_1}{\lambda(\varsigma_0)}\breve{S}(\varsigma_0)(T - \Theta_1) - \frac{d\varsigma_0}{ds}\frac{\partial T}{\partial s}, \tag{4}$$

$$\text{if} \quad \varsigma = \varsigma_k, \quad \text{then} \quad \frac{\partial T}{\partial \varsigma} = -\frac{\alpha_2}{\lambda(\varsigma_k)}\breve{S}(\varsigma_k)(T - \Theta_2) + \frac{d\varsigma_k}{ds}\frac{\partial T}{\partial s}, \tag{5}$$

if $s = s_a$, then $$\frac{\partial T}{\partial s} = \frac{\alpha_3}{\lambda}(T - \Theta_3), \tag{6}$$

if $s = s_b$, then $$\frac{\partial T}{\partial s} = -\frac{\alpha_4}{\lambda}(T - \Theta_4), \tag{7}$$

where $\breve{S}(\varsigma) = \sqrt{1 + (d\varsigma / ds)^2}$, $\Theta_i = \Theta_i(s, \varsigma, t)$, $\alpha_i = \alpha_i(s, \varsigma, t)$ $(i = 1, \ldots, 4)$ are the environment temperatures near the corresponding surfaces and the heat-transfer factors.

Equation (1) can be solved using the finite-difference method and the explicit time difference scheme. To this end, we apply uniform meshes along the meridian and over thickness to the meridional section of each link. The time derivative in (1) is given by

$$\frac{\partial T}{\partial t} = \frac{T(t + \Delta t) - T(t)}{\Delta t},$$

then

$$\tilde{T} = T(t + \Delta t) = T(t) + a\Delta t[F^{(s)}(t) + F^{(\varsigma)}(t)]. \tag{8}$$

The derivatives with respect to spatial coordinates in (2) are approximated by finite differences of the second order. After the discretization of the thermal conduction equation (1), we obtain a relation for determining the temperatures at the nodal points of the finite-difference mesh of the meridional section of the shell. In the same way, we obtain expressions [1] for the boundary conditions.

To obtain stable results with the above formulas, it is necessary that the coefficient of $T_{i,j}$ on the right-hand side of Eq. (8) be nonnegative after substituting the difference approximations of the derivatives in (4)–(7) for the boundary points. Here, the index *i* refers to the meridian, and *j* to the thickness of the shell. This condition leads to the following restriction for the time step:

$$\Delta t < \min(\tau_1, \tau_2, \tau_3, \tau_4), \tag{9}$$

where τ_k $(k = 1, \ldots, 4)$ are the parameters typical for each of the shell surfaces. To obtain the time step at which the calculation process is stable, beyond-boundary points are introduced for the shell surfaces. In particular, to obtain τ_1 on the inner surface from the boundary condition (4), we obtain an expression for the temperature $T_{i,0}$ at a beyond-boundary point:

$$T_{i,0} = T_{i,2} - 2\Delta\varsigma_{i,1}\left\{\frac{\breve{S}(\varsigma_0)}{\lambda_{i,1}}\Big[\alpha_{1i}(T_{i,1} - \theta_{1i}) + C\varepsilon_{1i}(T_{i,1} - \theta_{1i})(T_{i,1} + \theta_{1i})\Big(T_{i,1}^2 + \theta_{1i}^2\Big) - q_{1i}\Big] + \frac{d\varsigma_0}{ds}\frac{T_{i+1,1} - T_{i-1,1}}{2\Delta s_l}\right\}. \tag{10}$$

Introducing the reduced heat transfer coefficient

$$\alpha'_{1i} = \alpha_{1i} + C\bar{\varepsilon}_{1i}(\bar{T}_{i,1} + \bar{\theta}_{1i})(\bar{T}_{i,1}^2 + \bar{\theta}_{1i}^2), \tag{11}$$

and substituting (10) and (11) into (8) from the expression for the coefficient of $T_{i,j}$, we obtain τ_1:

$$\tau_1 = a_{i,1}^{-1}\left[\frac{2}{\Delta s^2} + \frac{2}{\Delta\varsigma_{1i}^2} + \frac{\alpha'_{1i}}{\lambda_{i,1}}\breve{S}_l(\varsigma_0)\left(\frac{7\lambda_{i,1} - 4\lambda_{i,2} + \lambda_{i,3}}{2\Delta\varsigma_{1i}\lambda_{i,1}} - k_i\right)\right]^{-1}. \tag{12}$$

In (11), the overbars indicate quantities known from the previous time step. Expression (12) coincides with the expression in [1] if α_{1i} is replaced by α'_{1i}. To obtain the parameters τ_k $(k = 2, 3, 4)$, we use the formulas from [1] replacing α_{ki} by α'_{ki}, where the latter is determined similarly to (11).

Thus, at each time step, the temperature at each point of the mesh is found using the recurrent procedure (8), the time step being determined from condition (9).

3. Determination of the Axisymmetric Thermoelastoplastic Stress–Strain State of the Shell under Repeated Loading and Assessment of Strength. The axisymmetric SSS of a shell under repeated loading is determined using a geometrically linear quasistatic problem statement after solving the heat conduction problem.

The deformation of the material is described by the modified theory of deformation processes along paths of small curvature [6, 11, 12], which is widely used to solve boundary-value problems of thermoplasticity [14–16, 19, 23] and to determine the destructive load for shells that model rocket elements [13, 20, 21]. In the case of active loading, these equations are identical to the equations of the flow theory [18, 24] associated with the Mises yield condition. We will use the equations of the modified theory of processes of small curvature linearized by the method of additional stresses [10, 15, 22]. Then the relationship of the components of the stress σ_{ij} and strain ε_{ij} tensors in the general case of an orthogonal curvilinear coordinate system has the form of Hooke's law with additional stresses:

$$\sigma_{ij} = 2G\varepsilon_{ij} + 3\lambda\varepsilon_0\delta_{ij} - \sigma_{ij}^{(D)}, \tag{13}$$

where

$$\sigma_{ij}^{(D)} = 2G(e_{ij}^{(P)}) + K\varepsilon_T\delta_{ij}, \tag{14}$$

$$\lambda = \frac{2G\nu}{1-2\nu}, \qquad \varepsilon_T = \alpha_T(T - T_0), \qquad K = \frac{E}{1-2\nu},$$

$$E = 2G(1+\nu), \qquad \delta_{ij} = \begin{cases} 1, & i = j, \\ 0, & i \neq j, \end{cases} \tag{15}$$

where $e_{ij}^{(p)} = \varepsilon_{ij}^{(p)}$ are the plastic strains; E, G, ν, and α_T are, respectively, the elastic modulus, shear modulus, Poisson's ratio, and linear thermal expansion coefficient dependent on temperature T; $\varepsilon_0 = \varepsilon_{ii}/3$ is the first invariant of the strain tensor linearly related to the first invariant of the stress tensor $\sigma_0 = \sigma_{ii}/3$ as

$$\sigma_0 = K(\varepsilon_0 - \varepsilon_T). \tag{16}$$

The SSS of an axisymmetrically loaded thin shell in the absence of torsion is described by the stress, $\sigma_{ss}, \sigma_{\theta\theta}$, and strain, ε_{ss}, $\varepsilon_{\theta\theta}, \varepsilon_{\varsigma\varsigma}$, components. Then Eqs. (13) have the form

$$\begin{aligned} \sigma_{ss} &= A_{11}\varepsilon_{ss} + A_{12}\varepsilon_{\theta\theta} - A_{1D}, \\ \sigma_{\theta\theta} &= A_{12}\varepsilon_{ss} + A_{22}\varepsilon_{\theta\theta} - A_{2D}, \end{aligned} \tag{17}$$

where

$$A_{11} = A_{22} = \frac{E}{1-\nu^2}, \qquad A_{12} = \nu A_{11},$$

$$A_{1D} = A_{11}(e_{ss}^{(p)} + \nu e_{\theta\theta}^{(p)}) + A_{11}(1+\nu)\varepsilon_T,$$

$$A_{2D} = A_{11}(e_{\theta\theta}^{(p)} + \nu e_{ss}^{(p)}) + A_{11}(1+\nu)\varepsilon_T. \tag{18}$$

Expressions (18) contain the plastic strains $e_{ss}^{(p)} = \varepsilon_{ss}^{(p)}$, $e_{\theta\theta}^{(p)} = \varepsilon_{\theta\theta}^{(p)}$, $\varepsilon_{\varsigma\varsigma}^{(p)} = -(\varepsilon_{ss}^{(p)} + \varepsilon_{\theta\theta}^{(p)})$, which are calculated at an arbitrary Mth stage as sums of increments Δ:

$$\varepsilon_{ss}^{(p)} = \sum_{m=1}^{M} \Delta_m \varepsilon_{ss}^{(p)}, \qquad \Delta_m \varepsilon_{ss}^{(p)} = \langle c_{ss} \rangle_m \Delta_m \Gamma_p,$$

$$\langle c_{ss}\rangle_m = \left\langle \frac{2\sigma_{ss} - \sigma_{\theta\theta}}{S} \right\rangle_m \qquad (s,\ \theta), \tag{19}$$

where the angle brackets denote averaging over a stage; S is the intensity of tangential stresses,

$$S = \left[\frac{1}{3}(\sigma_{ss}^2 - \sigma_{ss}\sigma_{\theta\theta} + \sigma_{\theta\theta}^2)\right]^{1/2}, \tag{20}$$

Γ_p is the intensity of accumulated plastic shear strain;

$$\Gamma_p = \sum_{m=1}^{M-1} \Delta_m \Gamma_p + \Delta_M \Gamma_p. \tag{21}$$

To determine $\Delta_M \Gamma_p$, we assume that the intensity of tangential stresses S (20), the intensity of shear strains,

$$\Gamma = \sqrt{\left[(\varepsilon_{ss} - \varepsilon_{\theta\theta})^2 + (\varepsilon_{\theta\theta} - \varepsilon_{\varsigma\varsigma})^2 + (\varepsilon_{\varsigma\varsigma} - \varepsilon_{ss})^2\right] / 6}$$

and temperature T are related by

$$S = \Phi(\Gamma,\ T). \tag{22}$$

To specify dependence (22), we use $\sigma \sim \varepsilon$ curves (σ is the stress, ε is the longitudinal strain of the sample) drawn based on data of tension tests on cylindrical samples at different fixed temperatures. For intermediate temperatures, these curves are obtained by interpolation. The transformation formulas between σ and ε and the second invariants of the stress and strain deviators are the following [16, 11, 22]:

$$S = \frac{\sigma}{\sqrt{3}}, \qquad \Gamma = \frac{S}{2G} + \Gamma_p, \qquad \Gamma_P = \frac{\sqrt{3}}{2}\left(\varepsilon - \frac{\sigma}{E}\right). \tag{23}$$

We assume that $\Gamma = \dfrac{S}{2G} + \Gamma_p^{(1)}$ during elastic unloading, where $\Gamma_p^{(1)}$ is the intensity of accumulated plastic shear strain (21) at the moment of unloading.

In the case where unloading is accompanied by secondary plastic deformation, we use the dependence

$$S = \Phi_1(\Gamma, \Gamma_p^{(1)}, T). \tag{24}$$

Dependence (24) is determined using (22), $\Gamma_p^{(1)}$, and the value of $S^{(1)}$ at the moment of unloading. In the case of reloading, we use the dependence

$$S = \Phi_2(\Gamma, \Gamma_p^{(2)}, T). \tag{25}$$

To specify dependence (25), we use (22), $\Gamma_p^{(2)}$ and the value of $S^{(2)}$ at the moment of unloading in the region of secondary plastic deformaiton. When specifying dependences (24) and (25), we take into account the Bauschinger effect:

$$S^{(1)} + S_T^{(2)} = S^{(2)} + S_T^{(3)} = 2S_T^{(1)}, \tag{26}$$

where $S_T^{(1)}, S_T^{(2)}, S_T^{(3)}$ are the intensities of tangential stresses corresponding to the yield points in (22), (24), (25), respectively. One of the methods of specifying dependences (24), (25) is described in [10]. Some approaches to accounting for secondary plastic deformation are described in [14, 19].

Thus, when determining the increment $\Delta_M \Gamma_p$ for the current loading stage, we use one of dependences (22), (24), (25) in each approximation.

We use formulas (17) to find the relationship between the forces N_s, N_θ, moments M_s, M_θ, and strains and changes in the curvature ε_s, ε_θ, κ_s, κ_θ of the coordinate surface of the shell:

$$N_s = C_{11}^{(0)}\varepsilon_s + C_{12}^{(0)}\varepsilon_\theta + C_{11}^{(1)}\kappa_s + C_{12}^{(1)}\kappa_\theta - N_{1D}^{(0)},$$

$$N_\theta = C_{12}^{(0)}\varepsilon_s + C_{22}^{(0)}\varepsilon_\theta + C_{12}^{(1)}\kappa_s + C_{22}^{(1)}\kappa_\theta - N_{2D}^{(0)},$$

$$M_s = C_{11}^{(1)}\varepsilon_s + C_{12}^{(1)}\varepsilon_\theta + C_{11}^{(2)}\kappa_s + C_{12}^{(2)}\kappa_\theta - N_{1D}^{(1)},$$

$$M_\theta = C_{12}^{(1)}\varepsilon_s + C_{22}^{(1)}\varepsilon_\theta + C_{12}^{(2)}\kappa_s + C_{22}^{(2)}\kappa_\theta - N_{2D}^{(1)}, \tag{27}$$

where

$$C_{mn}^{(j)} = \int_{\varsigma_0}^{\varsigma_k} A_{mn}\varsigma^j d\varsigma, \quad N_{mD}^{(j)} = \int_{\varsigma_0}^{\varsigma_k} A_{mD}\varsigma^j d\varsigma \quad (m,n = 1, 2,\ j = 0, 1, 2). \tag{28}$$

Relations (27), (28) together with the equilibrium and kinematic equations [7] form a system of 12 equations, which is reduced to a system of six ordinary differential equations with respect to the unknown functions $N_s, Q_s, M_s, u, w, \vartheta_s$, where Q_s is the shearing force; u, w are the displacements of points of the coordinate surface in the meridional and normal directions; ϑ_s is the angle of rotation of the normal to the coordinate surface. This system has the form

$$\frac{d\vec{Y}}{ds} = P(s)\vec{Y} + \vec{f}(s) \tag{29}$$

under the boundary conditions

$$B_1\vec{Y}(s_a) = \vec{b}_1, \quad B_2\vec{Y}(s_b) = \vec{b}_2, \tag{30}$$

where $\vec{Y}$ is the column vector of unknown functions; $\vec{Y} = \{N_s, Q_s, M_s, u, w, \vartheta_s\}$; $P(s)$ is the matrix of the system; $\vec{f}(s)$ is the column vector of additional terms; B_1, B_2 are given matrices, $\vec{b}_1, \vec{b}_2$ are given column vectors of boundary conditions. The nonzero elements of the matrix $P(s)$ are calculated by the formulas

$$p_{11} = -\frac{\cos\varphi}{r}(1+\lambda_1), \quad p_{13} = -\frac{\cos\varphi}{r}\lambda_2, \quad p_{14} = \frac{\cos^2\varphi}{r^2}(\lambda_1 C_{12}^{(0)} + C_{22}^{(0)} + \lambda_2 C_{12}^{(1)}),$$

$$p_{15} = p_{14}\tan\varphi, \quad p_{16} = -\frac{\cos^2\varphi}{r^2}(\lambda_3 C_{12}^{(0)} + \lambda_4 C_{12}^{(1)} - C_{22}^{(1)}),$$

$$p_{21} = \frac{1}{R_s} - \frac{\lambda_1\sin\varphi}{r}, \quad p_{22} = -\frac{\cos\varphi}{r}, \quad p_{23} = -\frac{\sin\varphi}{r}\lambda_2,$$

$$p_{24} = p_{15}, \quad p_{25} = p_{15}\tan\varphi, \quad p_{26} = p_{16}\tan\varphi,$$

$$p_{31} = -p_{22}\lambda_3, \quad p_{32} = -1, \quad p_{33} = -\frac{\cos\varphi}{r}(1-\lambda_4),$$

$$p_{34} = \frac{\cos^2\varphi}{r^2}(\lambda_1 C_{12}^{(1)} + C_{22}^{(1)} + \lambda_2 C_{12}^{(2)}), \quad p_{35} = p_{34}\tan\varphi,$$

$$p_{36} = -\frac{\cos^2\varphi}{r^2}(\lambda_3 C_{12}^{(1)} - C_{22}^{(2)} + \lambda_4 C_{12}^{(2)}), \quad p_{41} = \frac{C_{11}^{(2)}}{\delta_1}, \quad p_{43} = -\frac{C_{11}^{(1)}}{\delta_1},$$

$$p_{44} = -\lambda_1 p_{22}, \quad p_{45} = -p_{21}, \quad p_{46} = -p_{31}, \quad p_{54} = -p_{12},$$

$$p_{56} = -1, \quad p_{61} = p_{43}, \quad p_{63} = \frac{C_{11}^{(0)}}{\delta_1}, \quad p_{64} = -p_{13},$$

$$p_{65} = -p_{23}, \quad p_{66} = \lambda_4 p_{22}, \tag{31}$$

where

$$\lambda_1 = (C_{11}^{(1)} C_{12}^{(1)} - C_{12}^{(0)} C_{11}^{(2)}) / \delta_1, \quad \lambda_2 = (C_{11}^{(1)} C_{12}^{(0)} - C_{12}^{(1)} C_{11}^{(0)}) / \delta_1,$$

$$\lambda_3 = (C_{11}^{(2)} C_{12}^{(1)} - C_{12}^{(2)} C_{11}^{(1)}) / \delta_1, \quad \lambda_4 = (C_{11}^{(0)} C_{12}^{(2)} - C_{12}^{(1)} C_{11}^{(2)}) / \delta_1,$$

$$\delta_1 = C_{11}^{(0)} C_{11}^{(2)} - (C_{11}^{(1)})^2.$$

The nonzero components of the vector $\vec{f}(s)$ are expressed as

$$f_1 = -\frac{\cos\varphi}{r} [\lambda_1 N_{1D}^{(0)} + \lambda_2 N_{1D}^{(1)} + N_{2D}^{(0)}] - q_s, \quad f_2 = -\frac{\sin\varphi}{r} [\lambda_1 N_{1D}^{(0)} + \lambda_2 N_{1D}^{(1)} + N_{2D}^{(0)}] - q_\varsigma,$$

$$f_3 = \frac{\cos\varphi}{r} [\lambda_3 N_{1D}^{(0)} + \lambda_4 N_{1D}^{(1)} - N_{2D}^{(0)}], \quad f_4 = \frac{C_{11}^{(2)} N_{1D}^{(0)} - C_{11}^{(1)} N_{1D}^{(1)}}{\delta_1},$$

$$f_6 = -\frac{C_{11}^{(1)} N_{1D}^{(0)} - C_{11}^{(0)} N_{1D}^{(1)}}{\delta_1}, \tag{32}$$

where q_s, q_ς are the components of the distributed mechanical load.

From formulas (28) and (31), it follows that the elements of the matrix $P(s)$ are calculated using the geometrical parameters of the shell and the elastic characteristics of the material, which depend on the temperature at the current stage, and elements (32) of the vector $\vec{f}(s)$ depend on temperature through the external loads and plastic strains; the latter should be calculated by the method of successive approximations.

These relations make it possible to determine the SSS of the shell at any stage of loading. To carry out calculations, it is necessary to use data that describe the geometry of the shell, the boundary and loading conditions, and the material characteristics (curves $\sigma \sim \varepsilon$, Poisson's ratios, and linear thermal expansion coefficient depending on temperature). It is convenient to select stages so that the shell deforms elastically in the first stage.

In the first approximation, we assume that the plastic strains are equal to zero in (18) in the first stage of loading, that is, we solve the problem of thermoelasticity. In the subsequent stages, we use the values of the plastic strains (19) obtained at the previous stage in the first approximation and the values obtained in the previous approximation in the subsequent approximations. These values are necessary to calculate the elements of the column vector $\vec{f}(s)$ (32), while the elements of the matrix $P(s)$ (31) are found using the given temperature-dependent characteristics of the material; they do not change during successive approximations at this stage. Calculating the elements of the matrix $P(s)$ and the elements of the column vector $\vec{f}(s)$, we solve the boundary-value problem (29), (30) by reducing it to Cauchy problems, which are solved by the Runge–Kutta method with discrete orthogonalization [4].

After finding the unknown functions as a result of solving the boundary-value problem, we find the strain components and then the stress components (17).

Next, we calculate

$$\Delta_M \Gamma_p = \sum_{i=1}^{L-1} \Delta_{Mi} \Gamma_p + \Delta_{ML} \Gamma_p,$$

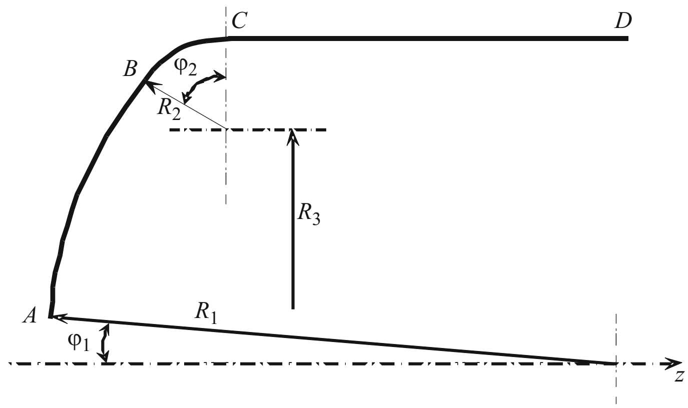

Fig. 1

$$\Delta_{ML}\Gamma_p = \frac{S - S^{(d)}}{2G}, \tag{33}$$

where L is the number of the current approximation in the M-th stage. The value of S in (33) is calculated by formula (20), and $S^{(d)}$ is determined by one of formulas (22), (24), and (25). Dependence (22) is used for the initial active load. If $\Delta\Gamma_p > 0$, then active load occurs; otherwise, we have unloading, that is, we set $\Delta\Gamma_p = 0$ and we continue the calculation. In the case of unloading ($\Gamma < \Gamma_p$), we use dependence (24). Similarly, when unloading occurs in the region of secondary plastic deformation and $\Gamma > \Gamma_p$, we use dependence (25). The process of successive approximations at a stage is terminated once

$$|\Delta_{ML}\Gamma_p| \le \delta, \tag{34}$$

where δ is a small predetermined number that describes the accuracy of solving the plasticity problem.

Solving the thermoplasticity problem at an arbitrary stage of loading, we use the components of the SSS of the shell to test the failure criteria. The external load under which

$$\sigma_e = \sigma_n, \tag{35}$$

where σ_e is the equivalent stress, and σ_n is the ultimate strength of the material at the temperature of this element of the shell, is considered the destructive load. We take the following expressions as the equivalent stress:

(i) maximum principal stress [8]

$$\sigma_e = \sigma_{\max}, \tag{36}$$

where $\sigma_{\max} = \max(\sigma_{ss}, \sigma_{\theta\theta})$.

(ii) the Sdobyrev criterion [9]

$$\sigma_e = (\sigma_i + \sigma_{\max})/2, \tag{37}$$

where σ_i is the stress intensity, $\sigma_i = S\sqrt{3}$, S is determined using formula (20);

(iii) the Mises criterion

$$\sigma_e = \sigma_i. \tag{38}$$

In the case of cyclic loading of the shell, it is possible to predict the number of cycles to failure from the change in plastic hysteresis or the strain range using the Coffin–Manson low-cycle fatigue criterion, as in [20].

4. Numerical Results. Let us determine the thermoplastic SSS of a shell that models a structural member under repeated high pressure. Figure 1 shows the meridian of the coordinate surface.

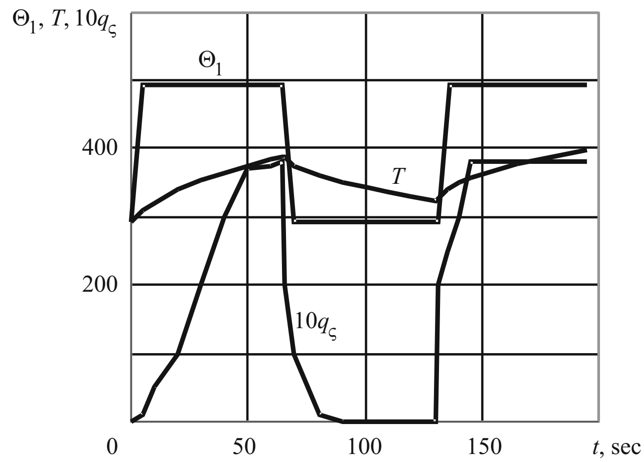

Fig. 2

TABLE 1

Stage No.	1	3	7	8	9	11	12	16	17	20	25
t, sec	5	20	60	65	99	80	90	130	131	145	195
q_ς, MPa	1	10	37.5	38	20	1	0	0	20	38	38

The shell is composed of spherical AB, toroidal BC, and cylindrical CD links smoothly connected to each other. The geometrical dimensions are as follows: $R_1 = 0.32$ m, $R_2 = 0.08$ m, $R_3 = 0.12$ m, $\varphi_1 = \pi / 50$, $\varphi_2 = \pi / 3$; the meridian length of the cylindrical link $L = 0.15$ m, the thickness of the shell $h = 0.01$ m.

The shell is made of EI 437 alloy the thermophysical characteristics linearly dependent on temperature: thermal conductivity and thermal diffusivity, respectively, $\lambda = 40$ W/(m·K), $a = 1.115 \cdot 10^{-5}$ m^2/sec at $T = 293$ K and $\lambda = 29$ W/(m·K), $a = 8.082 \cdot 10^{-6}$ m^2/sec at $T = 573$ K.

Curves $\sigma \sim \varepsilon$ depending on the temperature are given in [11]. Poisson's ratios and linear thermal expansion coefficients were considered independent of temperature: $\nu = 0.3$ and $\alpha_T = 12 \cdot 10^{-6}$ °C^{-1}. The ultimate strengths $\sigma_n = 980$ MPa and $\sigma_n = 926$ MPa at $T = 293$ K and $T = 573$ K, respectively [3].

The shell, which was initially unstressed and undeformed at $T_0 = 293$ K, is heated through convective heat exchange with the environment. The shell ends s_a and s_b are heat insulated ($\alpha'_3 = \alpha'_4 = 0$). The ambient temperature near the outer surface $\Theta_2 = 293$ K; the heat-transfer factor of this surface $\alpha'_2 = 200$ W/(m^2·K). The ambient temperature near the inner surface changes with time: $\Theta_1 = \Theta_1(t)$ (Fig. 2).

The temperature distribution over the meridional section of the shell was obtained by solving the thermal conduction problem using the above procedure. It was established that the temperature changes a little along the meridian and the thickness. The maximum temperature difference on the shell surfaces does not exceed 12 degrees. Figure 2 shows curves of temperature T versus time in the vicinity of the most heated element of the shell ($s = 0$, $\varsigma = -h / 2$).

The time-varying internal pressure q_ς MPa acts on the shell simultaneously with heating. Figure 2 shows the curves of pressure versus time.

The process of loading and heating of the shell is divided into 25 stages. The values of q_ς in some stages are given in Table 1 with the corresponding moments of time.

The boundary conditions on the edges of the shell are

$$\text{at} \quad s = s_a = 0 \qquad u = 0, \; w = 0, \; M_s = 0,$$

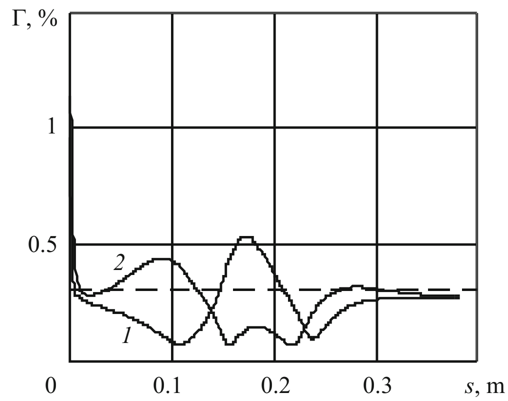

Fig. 3

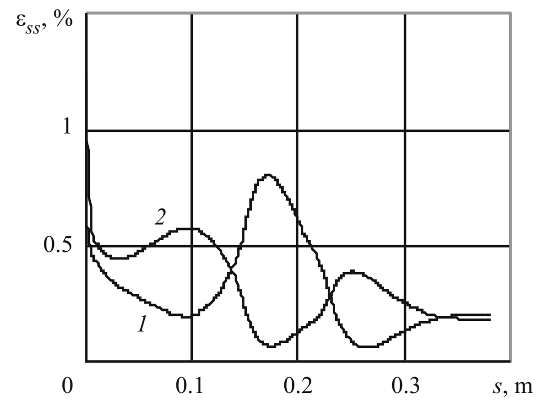

Fig. 4

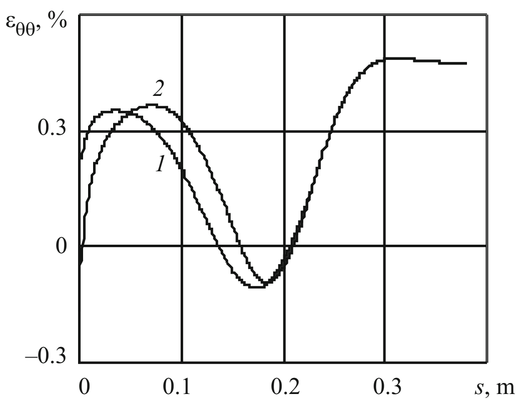

Fig. 5

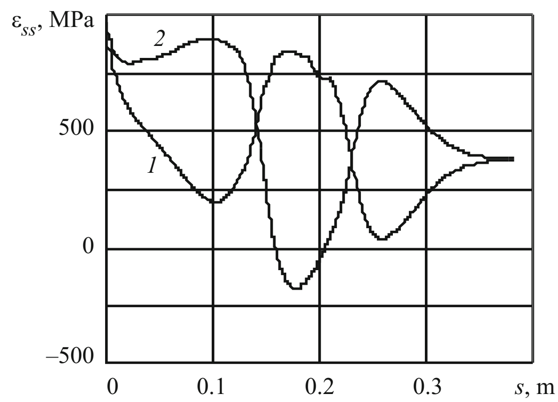

Fig. 6

at $s = s_b$ $$N_s = N_s^* = \frac{q_\varsigma (R_2 + R_3)}{2}, \; Q_s = 0, \; \vartheta_s = 0.$$

Figure 2 and Table 1 show that the mechanical load increases to the maximum in the 8th stage, decreases to zero in stages 12–16, and increases to the maximum again beginning from the 17th stage.

The maximum temperature is reached in stages 8 and 25, and the minimum temperature, in stages 11–16.

When solving the problem, we used 200 integration steps for each of the three links of the shell. The SSS was determined at 21 points over the thickness of the shell.

It was established that zones of plastic deformation appear in most of the shell in stages 1–8. Further, in the process of heating and loading in some elements of the shell, the active load changed to unloading, after that, active loading occurred again with increasing plastic deformations. Some calculated results for the 25th stage, that is, at the end of loading are shown in Figs. 3–10.

The zones of plastic deformation at the end of the process are shown in Fig. 3, which shows the change in the intensity of shear strains along the meridian. Numbers 1 and 2 in this and the subsequent figures refer to the inner and outer surfaces of the shell. The horizontal line shows the initial yield point of the material. Figures 4 and 5 show the change of the meridional and circumferential strains along the meridian, and Figs. 6 and 7 show the associated stresses.

The last figures show that the meridional stresses reach their maxima near the edge $s = s_a = 0$, and the circumferential stresses reach their maximuain the cylindrical part of the shell. Figure 8 shows the change of the intensity of shear strains along the meridian.

At each stage of loading, criteria (24)–(26) were tested after the completion of the process of successive approximations. In the 25th stage, criterion (24) is satisfied when the maximum meridional stress in the cross-section $s = s_a = 0$ is $\sigma_n = 975$ MPa when $q_\varsigma = 38$ MPa and $T = 399$ K.

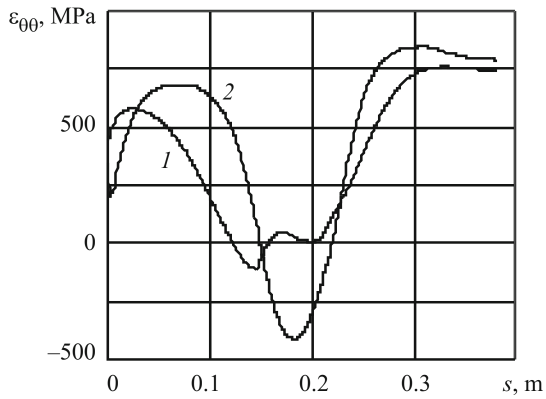

Fig. 7

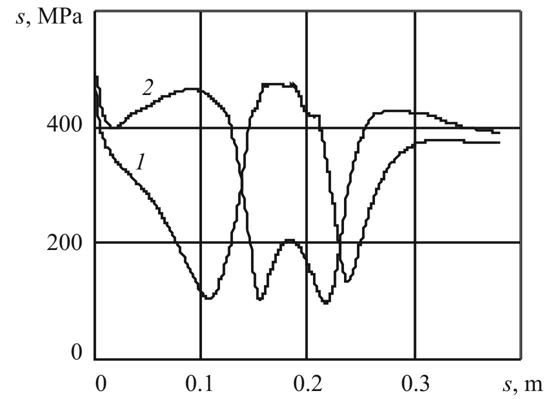

Fig. 8

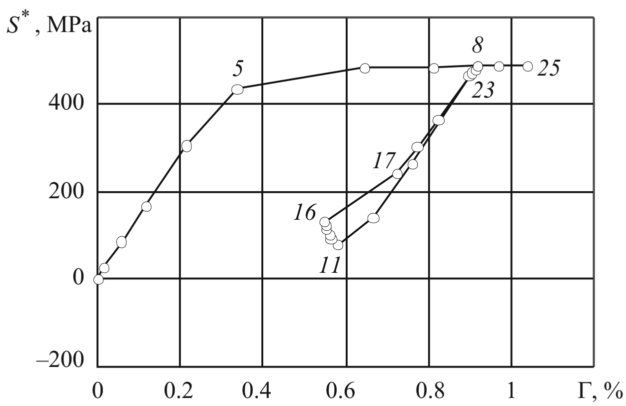

Fig. 9

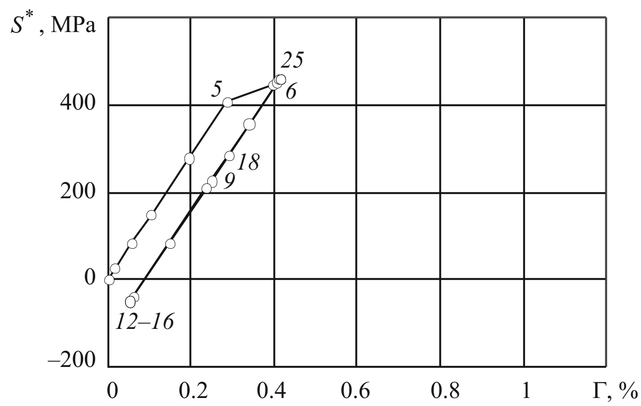

Fig. 10

During loading and heating, the direction of the process changed in some shell elements that deformed beyond the elastic limits: active loading, unloading, reloading with increase in the intensity of accumulated plastic strain.

Figure 9 shows curves $S^* \sim \Gamma$ for the point with coordinates $s = 0, \varsigma = -h/2$, where $S^* = \mathrm{sign}(\Gamma - \Gamma_p^{(1)}) \cdot S$ or $S^* = \mathrm{sign}(\Gamma - \Gamma_p^{(2)}) \cdot S$. The full circles indicate the ends of the stages, and the numbers are the stage numbers. Figure 9 shows that during repeated loading, the plastic strains increase compared with the initial load. Figure 10 shows similar results for the shell element near the point $s = 0.0737$ m, $\varsigma = h/2$. Here, the plastic strain occurred during the initial loading remains until the end of the process.

The calculations show that the SSS of the shell does not reach the destructive level under initial pressure $q_\varsigma = 38$ MPa. This level is reached during reloading when temperature $T = 399$ K in the most loaded elements of the shell.

Conclusions. A procedure for determining the stress–strain state and the destructive load of thin-walled structural members such as composite shells of revolution under repeated nonisothermal loading using an axisymmetric problem statement has been developed. It successively uses methods of solving the thermal conduction problem to determine the temperature and determining the elastoplastic stress–strain state of thin shells under thermomechanical loading, taking into account the loading history. Failure criteria known from the literature were used to determine the destructive load. The finite-difference method was used to solve the thermal conduction problem. The method of solving the thermoplasticity problem is based on the modified equations of the theory of isotropic deformation along paths of small curvature. The possibility of partial or complete unloading in the zones of plastic deformation and secondary plastic deformation has been taken into account. To this end, the previous effective algorithms and associated software for specifying the relationships between the second invariants of the stress and strain deviators in processes of variable thermomechanical loading have been improved taking into account the Bauschinger effect. A numerical example of solving problems of thermal conduction and thermoplasticity under variable repeated thermomechanical loading for a specific shell has been considered and the destructive load has been determined.

REFERENCES

1. A. Z. Galishin, P. A. Steblyanko, and Yu. N. Shevchenko, “Determining nonstationary temperature fields in thin laminated shells of revolution subject to axisymmetric heating,” *Mat. Probl. Tekhn. Mekh.*, No. 2(19), 3–12 (2012).
2. A. V. Lykov, *Theory of Thermal Conduction* [in Russian], Vysshaya Shkola, Moscow (1967).
3. N. N. Malinin, *Strength of Turbo Machines* [in Russian], Mashgiz, Moscow (1962).
4. Ya. M. Grigorenko and A. T. Vasilenko, *Theory of Shells with Variable Stiffness*, Vol. 4 of the five-volume series *Methods of Shell Design* [in Russian], Naukova Dumka, Kyiv (1981).
5. Yu. N. Shevchenko and I. V. Prokhorenko, *Theory of Elastoplastic Shells under Nonisothermal Loading*, Vol. 3 of the five-volume series *Methods of Shell Design* [in Russian], Naukova Dumka, Kyiv (1981).
6. Yu. N. Shevchenko and V. G. Savchenko, *Thermoviscoplasticity*, Vol. 2 of the five-volume series *Mechanics of Coupled Fields in Structural Members* [in Russian], Naukova Dumka, Kyiv (1987).
7. V. V. Novozhilov, *Thin Shell Theory*, Noordhoff, Groningen (1964).
8. G. S. Pisarenko, A. P. Yakovlev, and V. V. Matveev, *Strength of Materials* [in Russian], Naukova Dumka, Kyiv (1988).
9. V. P. Sdobyrev, “Long-term strength of EI 437B alloy in combined stress state,” *Izv. AN SSSR, OTN*, No. 4, 92–97 (1958).
10. Yu. N. Shevchenko, *Thermoplasticity under Variable Loading* [in Russian], Naukova Dumka, Kyiv (1970).
11. Yu. N. Shevchenko, M. E. Babeshko, and R. G. Terekhov, *Thermoviscoelastoplastic Processes of Combined Deformation of Structural Members* [in Russian], Naukova Dumka, Kyiv (1992).
12. Yu. N. Shevchenko, A. Z. Galishin, P. A. Steblyanko, M. V. Banias, P. G. Degtiarenko, and A. M. Tonkonozhenko, “Determining nonstationary temperature fields in thin laminated shells of revolution during combined heat exchange with the environment,” *Mat. Probl. Tekhn. Mekh.*, No. 2(25), 85–90 (2014).
13. M. E. Babeshko, A. Z. Galishin, A. I. Semenets, and Yu. N. Shevchenko, “Influence of the stress mode on the strength of high-pressure vessels,” *Int. Appl. Mech.*, **1**, No. 3, 319–325 (2015).
14. M. E. Babeshko and V. G. Savchenko, “Analyzing processes of nonisothermal loading of shells of revolution with allowance for repeated plastic strain,” *Int. Appl. Mech.*, **53**, No. 6, 639–646 (2017).
15. M. E. Babeshko and V. G. Savchenko, “Method of solving the problem of thermoradiation plasticity for layered axisymmetric bodies made of isotropic and orthotropic materials,” *Int. Appl. Mech.*, **57**, No. 3, 306–319 (2021).
16. M. E. Babeshko and V. G. Savchenko, “Elastoplastic axisymmetric stress–strain state of thin shells made of materials with different compressive and tensile moduli,” *Int. Appl. Mech.*, **57**, No. 4, 414–423 (2021).
17. H. S. Carslaw and J. C. Jaeger, *Conduction of Heat in Solids*, Oxford University Press, Oxford (1947).
18. R. Hill, *The Mathematical Theory of Plasticity*, Claredon Press, Oxford (1950).
19. M. E. Babeshko and V. G. Savchenko, “Technique of allowing for plastic strain under unloading in thermoplasticity problems for axisymmetric bodies,” *Int. Appl. Mech.*, **55**, No. 4, 416–425 (2019).
20. Yu. N. Shevchenko, N. F. Andrushko, M. E. Babeshko, M. V. Banyas, A. Z. Galishin, P. G. Dehtyarenko, V. G. Savchenko, A. V. Tonkonozhenko, and N. N. Tormakhov, “Development of mathematical models and computer technologies for the virtual destructive testing of shell structures,” *Sci. Innov.*, **9**, No. 6, 23–30 (2013).
21. Yu. N. Shevchenko, N. F. Andrushko, M. E. Babeshko, M. V. Banyas, A. Z. Galishin, P. G. Dehtyarenko, V. G. Savchenko, A. V. Tonkonozhenko, and N. N. Tormakhov, “Procedure of forecasting operation and extremal state of critical systems of the rocket technique under repeated thermo-force loading,” *Sci. Innov.*, **11**, No. 5, 25–36 (2015).
22. Yu. N. Shevchenko and V. G. Savchenko, “Three-dimensional problems of thermoviscoplasticity: focus on Ukrainian research (review),” *Int. Appl. Mech.*, **52**, No. 3, 217–271 (2016).
23. P. A. Steblyanko and Yu. N. Shevchenko, “Computational methods in stationary and nonstationary thermal-plasticity problems,” in: *Encyclopedia of Thermal Stresses* Vol. 2 C–D of 11-volume series, Springer, New York (2014), pp. 623–630.
24. M. Zyczkowski, *Combined Loadings in the Theory of Plasticity*, PWN, Warszawa (1981).